Fermilab

FERMILAB-Pub-03/258-A September 2003

Last modified July 4, 2003

The Richness-Dependent Cluster Correlation Function: Early SDSS Data

Neta A. Bahcall[1], Feng Dong[1], Lei Hao[1], Paul Bode[1], Jim Annis[2], James E. Gunn[1], Donald P. Schneider[3]

ABSTRACT

The cluster correlation function and its richness dependence are determined from over 10^3 clusters of galaxies – the largest sample of clusters studied so far – found in 400 deg^2 of Sloan Digital Sky Survey early data. The results are compared with previous samples of optically and X-ray selected clusters. The richness-dependent correlation function increases monotonically from an average correlation scale of $\sim 12\ h^{-1}$ Mpc for poor clusters with a mean separation of $\sim 20\ h^{-1}$ Mpc, to a correlation scale of ~ 20 - $25\ h^{-1}$ Mpc for the richer, more massive clusters with mean separations of ~ 60 - $90\ h^{-1}$ Mpc. X-ray selected clusters seem to suggest slightly stronger correlations than optically selected clusters but the results are consistent within 2-σ. The results are compared with large-scale cosmological simulations. The observed richness-dependent cluster correlation function is well represented by the standard flat LCDM model ($\Omega_m \simeq 0.3$, $h \simeq 0.7$), and, as expected, is inconsistent with the considerably weaker correlations predicted by $\Omega_m = 1$ models. We derive an analytic relation for the correlation scale versus cluster mean separation, $r_0 - d$, that best describes the LCDM prediction and the observations: r_0 (h^{-1} Mpc) $\simeq 2.6 \times d$ (h^{-1} Mpc) $^{0.5}$ (for $d \simeq 20$ - $90\ h^{-1}$ Mpc). Data from the complete Sloan Digital Sky Survey, when available, will greatly enhance the accuracy of the results and will allow a more precise determination of cosmological parameters.

Subject headings: cosmology:observations–cosmology:theory–cosmological parameters–dark matter–galaxies:clusters: general–large-scale structure of universe

[1]Princeton University Observatory, Princeton, NJ 08544

[2]Fermi National Accelerator Laboratory, P.O. Box 500, Batavia, IL 60510

[3]Department of Astronomy and Astrophysics, The Pennsylvania State University, University Park, PA 16802

1. Introduction

The spatial correlation function of clusters of galaxies and its dependence on richness provide powerful tests of cosmological models: both the amplitude of the correlation function and its dependence on cluster mass/richness are determined by the underlying cosmology. It has long been shown that clusters are more strongly correlated in space than galaxies, by an order-of-magnitude: the typical galaxy correlation scale, $\sim 5\ h^{-1}$ Mpc, increases to $\sim$ 20 - 25 h^{-1} Mpc for the richest clusters (Bahcall & Soneira 1983; Klypin & Kopylov 1983; see also Bahcall 1988; Huchra et al. 1990; Postman, Huchra, & Geller 1992; Bahcall & West 1992; Peacock & West 1992; Dalton et al. 1994; Croft et al. 1997; Abadi, Lambas, & Muriel 1998; Lee & Park 1999; Borgani, Plionis, & Kolokotronis 1999; Collins et al. 2000; Gonzalez, Zaritsky, & Wechsler 2002; and references therein). Bahcall & Soneira (1983) showed that the cluster correlation function is richness dependent: the correlation strength increases with cluster richness, or mass. The rarest, most massive clusters exhibit the strongest spatial correlations. Many observations have since confirmed these results (see references above), and theory has nicely explained them (Kaiser 1984; Bahcall & Cen 1992; Mo & White 1996; Governato et al. 1999; Colberg et al. 2000; Moscardini et al. 2000; Sheth, Mo, & Tormen 2001; and references therein). But the uncertainties in the observed cluster correlation function and its richness dependence – as manifested by the scatter among different measurements – have remained large.

In this paper we use the largest sample of clusters yet investigated, 1108 clusters selected from 379 deg^2 of early Sloan Digital Sky Survey data (see SDSS cluster catalog: Bahcall et al. 2003b), to determine the cluster correlation function. The SDSS and the cluster selection are described in §2. The large, complete sample of objectively selected clusters allows a new determination of the cluster correlation function and its richness dependence. The SDSS clusters in the current sample range from poor to moderately rich clusters; they are all in the redshift range $z = 0.1$ - 0.3.

We compare the newly determined SDSS cluster correlation function with results of previous samples of both optically and X-ray selected clusters (§4). We use large-scale cosmological simulations to compare the observational results with those expected from cosmological models (§5). The data are consistent with predictions from the standard flat LCDM model ($\Omega_m \sim 0.3$, $h \sim 0.7$), which best fits numerous other observations (e.g., Bahcall, Ostriker, Perlmutter, & Steinhardt 1999; Bennett et al. 2003; Spergel et al. 2003).

2. SDSS Cluster Selection

The Sloan Digital Sky Survey (SDSS; York et al. 2000) will provide a comprehensive digital imaging survey of 10^4 deg^2 of the North Galactic Cap (and a smaller, deeper area in the South) in five bands (u, g, r, i, z) to a limiting magnitude of r <23, followed by a spectroscopic multi-fiber survey of the brightest one million galaxies, to r <17.7, with a median redshift of $z \sim$0.1 (Fukugita et al. 1996; Gunn et al. 1998; Lupton et al. 2001; Hogg et al. 2001; Strauss, et al. 2002). For more details of the SDSS see Eisenstein et al. (2001); Blanton et al. (2002); Smith et al. (2002); Stoughton et al. (2002); and Pier et al. (2003).

Cluster selection was performed on 379 deg^2 of SDSS commissioning data, covering the area $\alpha(2000)$ = 355° to 56° and $\alpha(2000)$ = 145.3° to 236.0° at $\delta(2000)$= -1.25° to 1.25° (runs 94/125 and 752/756). The clusters studied in this paper were selected from these imaging data using a color-magnitude maximum-likelihood Brightest Cluster Galaxy method (maxBCG; Annis et al. 2003). The clusters are described in the SDSS cluster catalog of Bahcall et al. (2003b). The maxBCG method selects clusters based on the well-known color-luminosity relation of the brightest cluster galaxy (BCG) and the other E/S0 members. For each SDSS galaxy, a "BCG likelihood" is calculated based on the galaxy color ($g-r$ and $r-i$) and magnitude (M_i, in i-band). The BCG likelihood is then weighted by the number of nearby galaxies located within the color-magnitude region of the appropriate E/S0 ridgeline; this count, N_{gal}, includes all galaxies within 1 h^{-1} Mpc projected separation that are fainter than M_i and brighter than M_i(lim) = -20.25, and are located within 2-σ of the mean observed color scatter around the E/S0 ridgeline (i.e., $\pm^{0.1^m}_{0.15^m}$). The combined likelihood is used for cluster identification. The redshift that maximizes the cluster likelihood is adopted as the cluster redshift. Since BCG and elliptical galaxies in the red ridgeline possess very specific colors and luminosities, they provide excellent photometric redshift estimates for the parent clusters. The 1-σ uncertainty of the cluster redshift estimator is σ_z = 0.014 for $N_{gal}\geq$10 clusters and σ_z = 0.010 for the richer $N_{gal}\geq$20 clusters, where N_{gal} is the cluster richness defined above (see also Bahcall et al. 2003b).

In this paper we use all maxBCG clusters in the estimated redshift range z_{est} = 0.1 - 0.3 that are above a richness threshold of $N_{gal}\geq$ 10; this threshold corresponds to a typical cluster velocity dispersion of $\sigma_v \gtrsim$ 350 km s^{-1} (Bahcall et al. 2003b). The sample includes 1108 $N_{gal}\geq$10 clusters. Corrections for the selection function and false-positive detections for these relatively nearby clusters have been estimated from simulations and from visual inspection to be $\lesssim$ 10% (Bahcall et al. 2003b). The space-density of the $N_{gal}\geq$10 clusters is 5.3×10^{-5} h^3 Mpc^{-3}. To investigate the dependence of the correlation function on cluster richness, we break the sample into several richness subsamples with thresholds of $N_{gal}\geq$10, $\geq$13, $\geq$15, and $\geq$20. These samples include 1108, 472, 300, and 110 clusters, respectively.

3. The Cluster Correlation Function

The two-point spatial correlation function of clusters is determined by comparing the observed distribution of cluster pairs as a function of pair separation with the distribution of random catalogs within the same volume. The correlation function is estimated from the relation $\xi_{cc}(r) = F_{DD}(r)/F_{RR}(r) - 1$, where $F_{DD}(r)$ and $F_{RR}(r)$ are the frequencies of cluster-cluster pairs as a function of pair separation r in the data and in corresponding random catalogs, respectively. The random catalogs contain $\sim 10^3$ times the number of clusters in each data sample in order to reduce the statistical uncertainties. Clusters are randomly positioned on the sky in the random catalogs, covering the surveyed area. The redshifts of the random clusters are assigned following the redshift distribution of the observed clusters in order to minimize possible selection effects with redshift. The spatial correlation function is calculated in comoving coordinates. A flat LCDM cosmology with $\Omega_m = 0.3$ and a Hubble constant of $H_0 = 100\ h$ km s^{-1} Mpc^{-1} are used throughtout.

The uncertainty in the estimated cluster redshifts ($\sigma_z = 0.010$ for the richest $N_{gal} \geq 20$ clusters and $\sigma_z = 0.014$ for the $N_{gal} \geq 10$ to ≥ 15 clusters; §2) causes a small scattering effect in the cluster correlations, especially on small scales. We use Monte Carlo simulations to correct for this effect. We use simulations with a realistic cluster distribution with redshift and richness, convolve the clusters with the observed Gaussian scatter in redshift as given above, and determine the new convolved cluster correlation function. As expected, the redshift uncertainty causes a slight weakening – and flattening – of the true correlation function, especially at small separations, due to the smearing effect of the redshift uncertainty. We determine the correction factor for this effect as a function of scale r from 10^2 Monte Carlo simulations for each sample. The correction factor, which is found to be small (typically $\lesssim 20\%$), is then applied to the correlation function. An additional small correction factor due to false-positive detections is also estimated from Monte Carlo simulations. The false-positive detection rate is estimated to be negligible for the rich clusters with $N_{gal} \geq 15$; it is $5\% \pm 5\%$ for $N_{gal} \geq 13$, and $10\% \pm 5\%$ for $N_{gal} \geq 10$. The correlation function uncertainties are determined from the Monte Carlo simulations. Each simulation contains the same number of clusters as the relevant data sample. The final uncertainties in the correlation function are a combination of the statistical uncertainties and the uncertainties due to the small correction factors in the redshift and false-positive corrections discussed above.

The correlation function is determined for clusters with richness thresholds of $N_{gal} \geq 10$, ≥ 13, ≥ 15, and ≥ 20. The space-densities of these clusters, after correction for the effect of redshift uncertainties discussed above (Bahcall et al. 2003a), are 5.3×10^{-5}, 2.2×10^{-5}, 1.4×10^{-5}, and $0.5 \times 10^{-5} h^3$ Mpc^{-3}, respectively. All clusters are at $z_{est} = 0.1$ - 0.3.

The correlation function of the four samples are presented in Figure 1. The best-fit

power-law relation, $\xi(r) = (\frac{r}{r_0})^{-\gamma}$, is shown for each sample. These best fits are derived for scales $r \lesssim 50\ h^{-1}$ Mpc. The power-law slope γ has been treated both as a free parameter and as a fixed value ($\gamma = 2$). The difference in the correlation scale r_0 for these different slopes is small ($\lesssim 2\%$), well within the measured uncertainty. For $N_{gal}\geq$10, $\geq$13, $\geq$15, and $\geq$20, we find best-fit values of $r_0 = 12.8 \pm 0.7$ ($\gamma = 1.7 \pm 0.1$), 15.0 ± 0.9 ($\gamma = 2.1 \pm 0.2$), 17.7 ± 1.6 ($\gamma = 1.7 \pm 0.2$), and 21.2 ± 2.8 ($\gamma = 2 \pm 0.3$), similar to the r_0 values obtained for $\gamma = 2$ (Table 1). We use a fixed slope of 2 for the best-fit results presented in Figure 1 and Table 1. The richness dependence of the cluster correlation function is discussed in §4.

4. The r_0 - d Relation

The richness dependence of the cluster correlation function is shown in Figure 2; it is presented as the dependence of the correlation scale r_0 on the cluster mean separation d (Bahcall & Soneira 1983; Szalay & Schramm 1985; Bahcall 1988; Croft et al. 1997; Governato et al. 1999; Colberg et al. 2000; and references therein). Cluster samples with intrinsically larger mean separations correspond to lower intrinsic cluster abundances ($n_{cl} = d^{-3}$) and thus to higher cluster richness and mass (applies of course only to complete samples).

We compare our results with those of previous cluster samples, both optically and X-ray selected (Figure 2). These include the correlation function of Abell clusters (Bahcall & Soneira 1983; Peacock & West 1992; Richness class $\geq$1; Richness = 0 clusters are an incomplete sample and should not be included); APM clusters (Croft et al. 1997); Edinburgh-Durham clusters (EDCC; Nichol et al. 1992); Las-Campanas clusters (LCRS; Gonzalez, Zaritsky, & Wechsler 2002); galaxy groups (2dF; Zandivarez, Merchan, & Padilla 2003); and X-ray selected clusters (REFLEX: Collins et al. 2000; and XBACS: Abadi, Lambas, & Muriel 1998; Lee & Park 1999). A summary of the results is presented in Table 1.

For proper comparison of different samples, we will use the same set of standard parameters in the relative r_0 - d plot comparison: all results correspond to a redshift $z \sim$0, correlation power-law slope 2, and all scales are in comoving units in the LCDM cosmology (Ω_m= 0.3).

Most of the cluster samples are at small redshifts, $z \lesssim 0.1$ (Table 1). The only exceptions are the current SDSS clusters ($z \simeq 0.1$ - 0.3), and the LCRS clusters ($z \simeq 0.35$ - 0.5). To convert the results to $z \sim 0$ we use large-scale cosmological simulations of an LCDM model (1000 h^{-1} Mpc box simulation) and determine the cluster correlation function as well as the r_0 - d relation at different redshifts from $z = 0$ to $z = 1$. Details of the simulations and cluster selection are given in Bode et al. (2001) and are briefly summarized in §5. The correlation

function is determined following the same algorithmic method used for the data. We find that while both r_0 and d increase with redshift for the same mass clusters, as expected, there is no significant change in the r_0 - d relation as the redshift changes from $z = 0$ to $z \sim 0.5$ (for the current range of observed separations d; Figure 2). The relative r_0 - d relation remains essentially unchanged ($\lesssim 3\%$), well within the observational uncertainties. We emphasize that the individual parameters, r_0 and d, are plotted at the given sample's measured redshift and power-law slope, as listed in Table 1; it is only the relative r_0 - d relation that remains essentially unchanged within the above redshift range.

Most of the cluster correlation functions (Table 1) have been determined to have a power-law slope in the range of $\sim 2 \pm 0.2$. The APM highest richness clusters report significantly steeper slopes (3.2, 2.8, 2.3); these samples also contain the smallest number of clusters (17, 29, 58). The correlation scale r_0 is inversely correlated with the power-law slope; a steeper slope is likely to yield a smaller correlation scale. The APM analysis (Croft et al. 1997) presents the best χ^2 fit for r_0 as a function of the slope γ. We use their best r_0 results for a slope of 2 for these richest APM clusters. Using cosmological simulations, we investigate the dependence of r_0 on the slope within the more typical observed range of 2 ± 0.2. For the current range of mean separations d we find only a small change in r_0 ($\lesssim 5\%$) when the slope changes within this observed range; this range includes all the data samples used (except for the APM samples above). The X-ray cluster sample XBACS yields similar correlation scales for slopes ranging from $\sim$ 1.8 to 2.5, as seen in the analysis of Abadi, Lambas, & Muriel (1998) and Lee & Park (1999). Similarly, the SDSS correlation scales are nearly the same when using a free slope fit (typically 1.7 to 2.1) or a fixed slope of 2 (§3). Since most of the observations are reported with a slope of 2, we adopt the latter as the standard slope for the results presented in figure 2. The only correction applied is to the three highest richness APM subsamples described above; we show these subsamples both with and without the correction. We also varify using cosmological simulations that the LCRS sample at $z \sim$ 0.35 - 0.55, with a slope of 2.15, has an r_0 - d relation consistent with the standard set of parameters used in Figure 2 ($z \sim 0$, slope $\gamma \sim 2$).

Finally, we convert all scales (r_0 and d from Table 1) to the same Ω_m=0.3 cosmology (LCDM). The effect of the cosmology on the overall observed r_0 - d relation is small ($\lesssim 3\%$), partly because Ω_m= 1 was used only at small redshifts ($z \lesssim 0.1$), where the effect is small, but also because the cosmology affects both r_0 and d in the same way; this causes only a minor relative change in the r_0 - d relation.

A comparison of all the results, including the minor corrections discussed above, is shown in Figure 2. Figure 2a presents all the results, including both optically and X-ray selected clusters; Figure 2b includes only the optically selected samples. The richness-dependance

of the cluster correlation function is clearly apparent in Figure 2. The rich X-ray clusters seem to suggest somewhat stronger correlations than the optically selected samples, but the difference is only at a $\lesssim$ 2-σ level. Improved samples of both optically and X-ray selected clusters should reduce the scatter and help address this important comparison.

5. Comparison with Cosmological Simulations

We compare the results with large-scale cosmological simulations of a standard LCDM model (Ω_m= 0.3, h = 0.67, σ_8 = 0.9), and a tilted SCDM model, TSCDM (Ω_m= 1, h = 0.5, n = 0.625, σ_8 = 0.5). The TPM high-resolution large-volume simulations (Bode et al. 2001) used 1.34×10^8 particles with an individual particle mass of $6.2 \times 10^{11} h^{-1}$ $M_\odot$; the periodic box size is 1000 h^{-1} Mpc for LCDM and 669 h^{-1} Mpc for TSCDM. The simulated clusters are ordered by their abundance based on cluster mass within 1.5 h^{-1} Mpc. The results of the cosmological simulations for the r_0 - d relation of $z = 0$ clusters are presented by the two bands in Figure 2 (1-σ range). A correlation function slope of 2 was used in the analysis, for proper comparison with the data. When used as a free parameter, the slope in the simulations is found to be within $\pm$10% of this value. The top band in Figure 2 represents LCDM and the lower band is TSCDM. Also shown, for comparison, are the simulations results of Colberg et al. (2000) for LCDM (dot-dash curve) and Governato et al. (1999) for a standard untilted SCDM (Ω_m= 1, h = 0.5, n = 1, σ_8 = 0.7; dotted line). The agreement among the simulations is excellent. As expected, the untilted SCDM model yields lower r_0's than the strongly tilted model TSCDM.

An analytic relation that approximates the LCDM r_0 - d relation (solid curve) is

$$\frac{r_0}{1h^{-1}Mpc} = 2.6 \times (\frac{d}{1h^{-1}Mpc})^{\,0.5} \qquad (for \;\; 20 \lesssim d \lesssim 90\ h^{-1}Mpc) \tag{1}$$

The observed richness-dependent cluster correlation function agrees well with the standard LCDM model. The correlation scales, and the r_0 - d relation, increase as $\Omega_m h$ decreases and the spectrum shifts to larger scales. The Ω_m= 1 models are inconsistent with the data, yielding considerably weaker correlations than observed. This fact has of course been demonstrated earlier; in fact, the strength of the cluster correlation function and it's richness dependence were among the first indications against the standard Ω_m= 1 SCDM model (Bahcall & West 1992; Croft et al. 1997; Borgani, Plionis, & Kolokotronis 1999; Governato et al. 1999; Colberg et al. 2000; and references therein).

The scatter in the observed r_0 - d relation among different samples is still large, es-

pecially when both the optical and X-ray selected samples are included. A high-precision determination of the cosmological parameters cannot therefore be achieved at this point. With more accurate data of both optical and X-ray selected clusters the scatter will decrease and a more precise determination of the cosmological parameters will be possible.

6. Conclusions

We determine the cluster correlation function and it's richness dependance using over 10^3 clusters of galaxies found in 379 deg^2 of the Sloan Digital Sky Survey early release data. The cluster correlation function shows a clear richness dependance, with increasing correlation strength with cluster richness/mass. The results are combined with previous samples of both optically and X-ray selected clusters, and compared with cosmological simulations. We find that the richness-dependent cluster correlation function is consistent with predictions from the standard flat LCDM model (Ω_m= 0.3, h = 0.7), and, as expected, inconsistent with the weaker correlations predicted by Ω_m= 1 models.

We derive an analytic relation for the correlation scale versus cluster mean separation relation, $r_0(d)$, that best describes the LCDM expectations and the observations; this is given by Equation 1. The correlation scales of the richest clusters are approximately 25 h^{-1} Mpc. X-ray selected clusters suggest somewhat stronger correlations than the optically selected clusters, but the results are consistent within 2-σ.

Future data from the Sloan Digital Sky Survey and from other large complete surveys will greatly enhance the accuracy of the derived cluster correlation function and allow a more precise measurement of cosmological parameters.

Funding for the creation and distribution of the SDSS Archive has been provided by the Alfred P. Sloan Foundation, the Participating Institutions, the National Aeronautics and Space Administration, the National Science Foundation, the U.S. Department of Energy, the Japanese Monbukagakusho, and the Max Planck Society. The SDSS Web site is http://www.sdss.org/. The SDSS is managed by the Astrophysical Research Consortium (ARC) for the Participating Institutions. The Participating Institutions are The University of Chicago, Fermilab, the Institute for Advanced Study, the Japan Participation Group, The Johns Hopkins University, Los Alamos National Laboratory, the Max-Planck-Institute for Astronomy (MPIA), the Max-Planck-Institute for Astrophysics (MPA), New Mexico State University, University of Pittsburgh, Princeton University, the United States Naval Observatory, and the University of Washington.

REFERENCES

Abadi, M., Lambas, D., & Muriel, H. 1998, ApJ, 507, 526

Annis, J., et al. 2003, in preparation.

Bahcall, N. A. & Soneira, R. M. 1983, ApJ, 270, 20

Bahcall, N. A. 1988, ARA&A, 26, 631

Bahcall, N. A. & West, M. J. 1992, ApJ, 392, 419

Bahcall, N. A. & Cen, R. 1992, ApJ, 398, L81

Bahcall, N. A., Ostriker, J. P., Perlmutter, S., & Steinhardt, P. J. 1999, Science, 284, 1481

Bahcall, N. A., Dong, F., Bode, P. et al. 2003a, ApJ, 585, 182

Bahcall, N. A. et al. 2003b, ApJS, vol.148 (October 2003), astro-ph/0305202

Bennett, C. L. et al. 2003, ApJ, in press

Blanton, M. R., Lupton, R .H. et al. 2003, AJ, 125, 2276

Bode, P., Bahcall, N. A., Ford, E. B., & Ostriker, J. P., 2001, ApJ, 551, 15

Borgani, S., Plionis, M., & Kolokotronis, V. 1999, MNRAS, 305, 866

Colberg, J. M. et al. 2000, MNRAS, 319, 209

Collins, C. et al. 2000, MNRAS, 319, 939

Croft, R. A. C. et al. 1997, MNRAS, 291, 305

Dalton, G. B. et al. 1994, MNRAS, 271, L47

Eisenstein, D.J., et al 2001, AJ, 122, 2267

Fukugita, M. et al. 1996, AJ, 111, 1748

Gonzalez, A. H., Zaritsky, D., Wechsler, R. H. 2002, ApJ, 571, 129

Governato, F. et al. 1999, MNRAS, 307, 949

Gunn, J. E. et al. 1998, AJ, 116, 3040

Hogg, D. W. et al. 2001, AJ, 122, 2129

Huchra, J., Henry, J. P., Postman, M., & Geller, M. 1990, ApJ, 365, 66

Kaiser, N. 1984, ApJ, 284, L9

Klypin, A. A. & Kopylov, A. I. 1983, Soviet Astron. Lett. 9, 41

Lee, S., Park, C. 1999, JKAS, 32, 1

Lupton, R., et al. 2001, ASP Conf. Ser.238, vol.10, 269

Mo, H. J. & White, S. D. M. 1996, MNRAS, 282, 347

Moscardini, L., Matarrese, S., Lucchin, F., Rosati, P. 2000, MNRAS, 316, 283

Nichol, R. C., Collins, C. A., Guzzo, L., & Lumsden, S. L. 1992, MNRAS, 255, 21

Peacock, J. A. & West, M. J. 1992, MNRAS, 259, 494

Pier, J. R. et al. 2003, AJ, 125, 1559

Postman, M., Huchra, J., & Geller, M. 1992, ApJ, 384, 404

Sheth, R. K., Mo, H. J., Tormen, G. 2001, MNRAS, 323, 1

Smith, J. A. et al. 2002, AJ, 123, 2121

Spergel, D. N. et al. 2003, ApJ, in press

Stoughton, C., et al. 2002, AJ, 123, 485

Strauss, M., et al. 2002, AJ, 124, 1810

Szalay, A. S. & Schramm, D. N. 1985, Nature, 314, 718

York, D. G. et al. 2000, AJ, 120, 1579

Zandivarez, A., Merchan, M. E., & Padilla, N. D. 2003, astro-ph/0303450

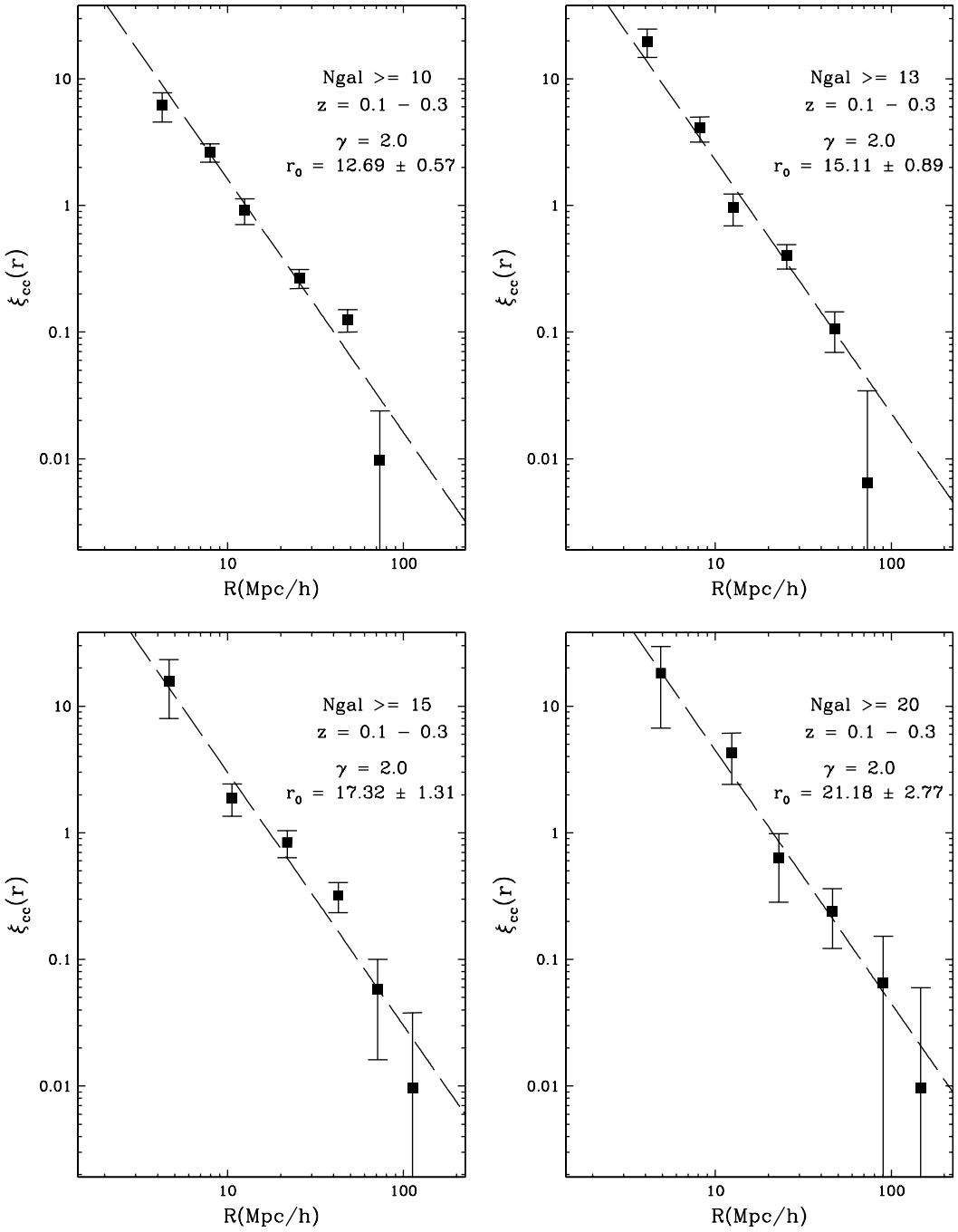

Fig. 1.— The SDSS cluster correlation function (z_{est} = 0.1 - 0.3) for four richness thresholds (N_{gal}≥10, ≥13, ≥15, ≥20). Best-fit power-laws with slope 2 are shown by the dashed lines; the correlation scales r_0 are listed in each panel (1-σ uncertainties).

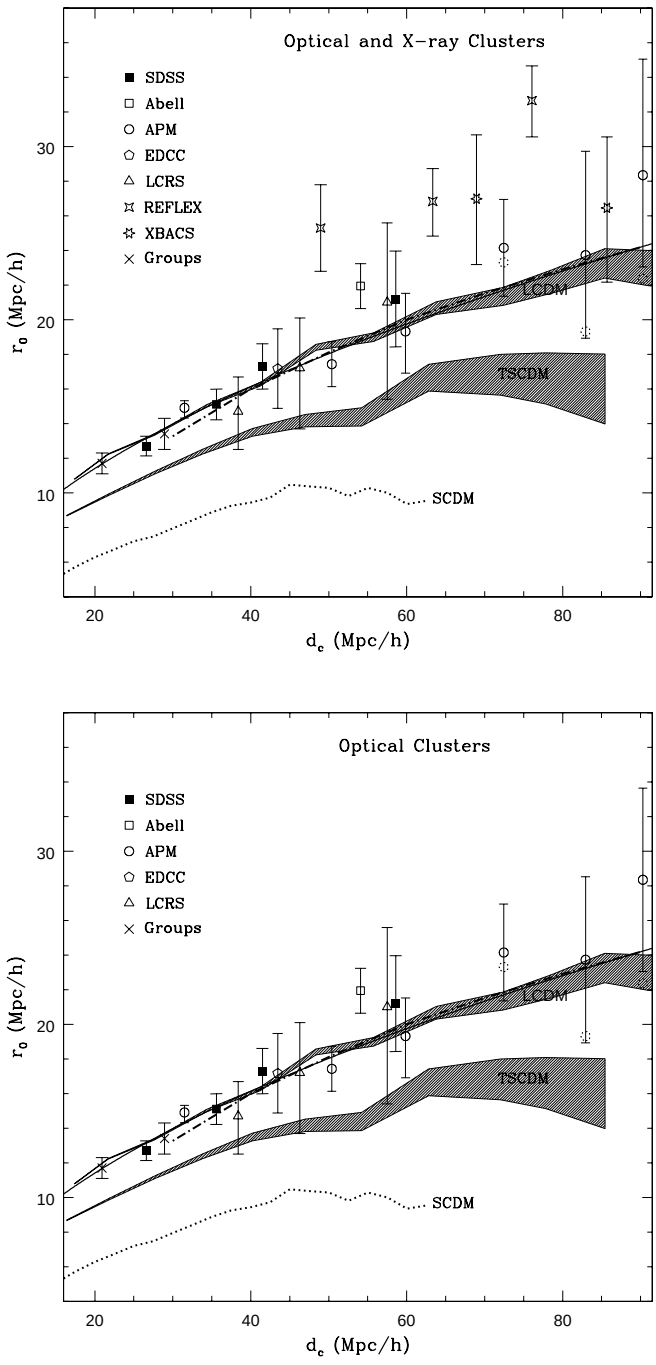

Fig. 2.— The richness dependence of the cluster correlation function: dependence of the correlation-scale r_0 on the mean cluster separation d. The data points (1-σ error-bars) are labeled in each Figure; a slope of $\sim$2 and LCDM comoving scales are used (see §4 and Table 1). Fig.2a includes all samples, both optical and X-ray clusters; Fig.2b presents optically selected clusters. Results of cosmological simulations (current paper) are shown by the two bands (LCDM and Tilted-SCDM). Previous simulations of LCDM (dot-dash curve) and untilted SCDM (dotted curve) are also shown (see §5). The solid curve is an analytic relation that best describes LCDM predictions and the data: $r_0 = 2.6\sqrt{d}$ (Equation 1).

Table 1. The Cluster Correlation Function*

Samples	Threshold	N_{cl}	z	γ	r_0 (h^{-1} Mpc)	d (h^{-1} Mpc)	Cosmology	References
SDSS	$N_{gal} \geq 10$	1108	0.1-0.3	2	12.7 ± 0.6	26.6	LCDM	this work
	$N_{gal} \geq 13$	472	0.1-0.3	2	15.1 ± 0.9	35.6	LCDM	this work
	$N_{gal} \geq 15$	300	0.1-0.3	2	17.3 ± 1.3	41.5	LCDM	this work
	$N_{gal} \geq 20$	110	0.1-0.3	2	21.2 ± 2.8	58.1	LCDM	this work
Abell	Rich ≥ 1	195	$\lesssim 0.08$	2	21.1 ± 1.3	52	SCDM	1,2
APM	R ≥ 50	364	$\sim$<0.1>	2.1	$14.2 \pm^{0.4}_{0.6}$	30	SCDM	3
	R ≥ 70	114	<0.1>	2.1	16.6 ± 1.3	48	SCDM	3
	R ≥ 80	110	<0.1>	1.7	$18.4 \pm^{2.2}_{2.4}$	57	SCDM	3
	R ≥ 90	58	<0.1>	2.3	22.2 ± 2.8	69	SCDM	3
				[2]	$[23.0 \pm 2.9]$**			
	R ≥ 100	29	<0.1>	2.8	18.4 ± 4.8	79	SCDM	3
				[2]	$[22.6 \pm 6.0]$**			
	R ≥ 110	17	<0.1>	3.2	21.3 ± 5.3	86	SCDM	3
				[2]	$[27.0 \pm 6.7]$**			
EDCC		79	$\lesssim 0.13$	2	16.2 ± 2.3	41	SCDM	4
LCRS		178	0.35-0.475	2.15	$14.7 \pm^{2.0}_{2.2}$	38.4	LCDM	5
		158	0.35-0.525	2.15	$17.2 \pm^{2.9}_{3.5}$	46.3	LCDM	5
		115	0.35-0.575	2.15	$20.9 \pm^{4.6}_{5.6}$	58.1	LCDM	5
REFLEX (X-ray)	$L_{X_{44}} \geq 0.08$	39	$\lesssim 0.05$	2	24.8 ± 2.5	48	SCDM	6
	$L_{X_{44}} \geq 0.18$	84	$\lesssim 0.075$	2	$25.8 \pm^{1.9}_{2.0}$	61	SCDM	6
	$L_{X_{44}} \geq 0.3$	108	$\lesssim 0.10$	2	$31.3 \pm^{2.0}_{2.1}$	72	SCDM	6
	$L_{X_{44}} \geq 0.5$	101	$\lesssim 0.125$	2	$25.8 \pm^{3.2}_{3.3}$	88	SCDM	6
XBACS (X-ray)	$L_{X_{44}} \geq 0.24$	49	$\lesssim 0.07$	1.8-2.5	25.7 ± 3.7	66	SCDM	7,8
	$L_{X_{44}} \geq 0.48$	67	$\lesssim 0.09$	1.8-2.5	25.2 ± 4.1	82	SCDM	7,8
	$L_{X_{44}} \geq 0.65$	59	$\lesssim 0.11$	1.6-2.2	$30.3 \pm^{8.2}_{6.5}$	98	SCDM	7,8
Groups (2dF)	$M_{vir} \geq 5e13$	920	<0.12>	2	11.7 ± 0.6	20.93	LCDM	9
	$M_{vir} \geq 1e14$	540	<0.13>	2	13.4 ± 0.9	28.93	LCDM	9

*Columns: 1)Sample; 2)Richness or X-ray luminosity (L_X in 10^{44} erg s^{-1}) or M_{vir} (in $M_\odot$) threshold; 3)Number of clusters in sample; 4)Redshift range or mean redshift; 5)Slope used in the correlation function; 6)Correlation scale (with 1-σ); 7)Cluster mean separation; 8)Cosmology used in the scale determinations [flat $\Omega_m \simeq 0.3$ (LCDM), or $\Omega_m = 1$ (SCDM)]; 9) References [1.Bahcall & Soneira 1983; 2.Peacock & West 1992; 3.Croft et al. 1997; (note that larger r_0's are obtained for APM by Lee & Park 1999); 4.Nichol et al. 1992; 5.Gonzalez, Zaritsky, & Wechsler 2002; 6.Collins et al. 2000; 7.Abadi, Lambas, & Muriel 1998; 8.Lee & Park 1999; 9.Zandivarez, Merchan, & Padilla 2003]

**Correlation scale r_0 using a slope of 2 (see §4)